# Investigation of IMD Asymmetry in Microwave FETs via Volterra Series

Paolo Colantonio, Franco Giannini, Ernesto Limiti, Antonio Nanni
Università di Roma Tor Vergata, Electronic Engineering Department,
via del Politecnico 1, 00133 Roma, ITALY, +(39) 06 72597351

***Abstract*** **— IMD asymmetry generation and its asymmetrical behaviour are discussed and clarified in this contribution using a Volterra series approach. The approach has been applied to a power PHEMT device for X-Band application. The effects of harmonic terminations have been clarified, stressing the relevance of baseband terminations and in particular of the output susceptance. Simplified expressions are inferred to clarify the effects of output terminations. Finally, the opportunity to choose a suitable fundamental and second harmonic output termination to reduce intermodulation asymmetry is discussed.**

## I. Introduction

Non linear distortion analysis and prediction in microwave circuits is an issue attracting many research efforts. One of the main aspects under study is the asymmetric amplitudes of lower- and upper-side-band Intermodulation Distortion (IMD) products, which are generated in a non linear device under two-tone driving excitations. Such phenomenon generates confusion or ambiguity during device characterisation and modelling, in the measurement of third-order intercept point ($IP_3$) and other distortion figures of merit. Moreover, IMD asymmetry has to be carefully accounted for in predistortion circuit design, due to different compensation requirements for lower and upper sidebands, if an in-band only scheme is adopted.

Many efforts have been devoted to investigate causes and mechanisms generating IMD asymmetries in active devices. In particular, the key role of base-band impedances or biasing networks on IMD performances have been focused and experimentally demonstrated [1,2]. From a theoretical point of view, to demonstrate the effects of loading impedances at different frequencies, the Volterra approach is usually adopted [3]. With the latter, the effects of circuit elements can be evidenced, focusing on the difference $\Delta H_3$ between the third-order transfer functions associated to lower $H_3(\omega_1,\omega_1,-\omega_2)$ and upper $H_3(\omega_2,\omega_2,-\omega_1,)$ Volterra kernels, assuming two input excitations at $\omega_1$ and $\omega_2$ ($\omega_2 > \omega_1$).

In this contribution, using the Volterra approach, the effects of base-band terminations on IMD asymmetry are analyzed, inferring symbolical expressions. Moreover, the relevance of base-band output load, and in particular of its susceptance, in the generation of IMD asymmetries, is stressed, as experimentally demonstrated in [4,5].

## II. Device Model

The proposed analysis of the IMD generation has been applied to a 1-mm (10x100µm) PHEMT power device by Alenia Marconi Systems. The device has been modelled through an equivalent-circuit approach, as depicted in Fig. 1, inferring both the extrinsic (linear) parasitic components and the intrinsic (boxed) non linear elements. The latter have been characterised using pulsed I-V and S-parameter measurements. In particular, non linear elements are represented by neural network functions [6].

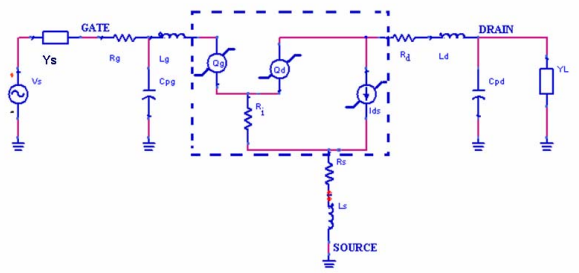


**Fig. 1:** Device non linear equivalent circuit used for the analysis.

To adopt the Volterra analysis, the non linear functions have been approximated through a polynomial series of input and output voltage signals, as follows:

$$i_{ds}(v_{gs}, v_{ds}) = \sum_n \sum_j G_{m_n d_j} v_{gs}^{\ n} v_{ds}^{\ j}. \quad (1)$$

$$Q_g(v_{gs}, v_{ds}) = \sum_n \sum_j C_{g_{n,j}} v_{gs}^{\ n} v_{ds}^{\ j} \quad (2)$$

$$Q_d(v_{gs}, v_{ds}) = \sum_n \sum_j C_{d_{n,j}} v_{gs}^{\ n} v_{ds}^{\ j}. \quad (3)$$

where $G$'s and $C$'s are the coefficients associated to the series expansion (truncated to the third order) of the non linear functions.

In order to analyse IMD asymmetry, two input signals at frequencies $f_1$ and $f_2$ are considered (with $f_2$= 9.6 GHz and $f_2 - f_1$= 30 MHz). The analysis here reported have been performed biasing the active device in Class AB condition (drain bias $V_{DD}$=8 V and gate bias $V_{GG}$=-0.4 V). Bias point selection clearly affects the numerical values of the results but does not impact the generality of the analysis.

*A. Full Non Linear Model*

By Volterra analysis, the first three kernels (i.e. non linear transfer functions) $H_i$ at the drain of the active device have been extracted. Such kernels are used to describe device performances (e.g. output power $P_{out}$, power added efficiency, PAE, and the distortion characteristics) in terms of both device equivalent circuit elements and input and output external loads ($Y_G$ and $Y_L$ in Fig. 1).

Firstly, assuming short-circuit condition for base-band terminations (representing the condition of an ideal LC bias network), no IMD asymmetry arises, as obtained via Harmonic Balance analysis and confirmed by the developed Volterra approach.

In the above condition, effects of harmonic terminations have been analysed through load pull simulations. The difference ($\Delta IM_3$) between the third order intermodulation component powers associated to the upper and lower sidebands, defined as :

$$\Delta IM_3 = \frac{1}{2}\left(\frac{3}{4}A^3\right)^2 \cdot \mathrm{Re}(Y_L) \cdot \Delta \qquad (4)$$

where

$$\Delta = \left|H_3(\omega_2,\omega_2,-\omega_1)\right|^2 - \left|H_3(\omega_1,\omega_1,-\omega_2)\right|^2 \qquad (5)$$

can be monitored. As summarised in Table 1, where the maximum $\Delta IM_3$ is reported, the effect of harmonic terminations becomes negligible.

| f | | 2f | | $\lvert\Delta IM_3\rvert$ [dB] |
|---|---|---|---|---|
| $\Gamma_{in}$ | $\Gamma_{out}$ | $\Gamma_{in}$ | $\Gamma_{out}$ | |
| 0 | Load pull | -1 | -1 | <0.1 |
| Load pull | 0 | -1 | -1 | <0.3 |
| 0 | 0 | -1 | Load pull | <0.06 |
| 0 | 0 | Load pull | -1 | <0.03 |

**Table 1:** IMD asymmetries determined assuming input and output base-band short-circuit terminations.

Secondly, to analyse the effects of base-band loads, second harmonic terminations have been assumed short-circuited, while the fundamental loads have been fixed to 50Ω. A load pull on both base-band input and output impedances has been therefore performed to analyse the relevance of such terminations independently. The resulting contour plots for $\Delta IM_3$ are reported in Fig. 2, assuming for the un-tuned port a base-band short-circuit condition. As it can be noted from Fig. 2b, IMD asymmetry is strongly dependent on output biasing network, resulting in a maximum difference of 10dB. Moreover, $\Delta IM_3$ reduces to zero if the base-band output termination is purely resistive. Therefore, the reactive part of the drain base-band termination (basically determined by the output bias network) is the main responsible of IMD asymmetry, while the effects of gate base-band termination are negligible when the output is shorted. Furthermore, $\Delta IM_3$ asymmetry exhibits an anti-symmetric behavior with inductive or capacitive terminations, with the former implying an higher IMD power at $2\omega_2-\omega_1$ (Fig. 2b).

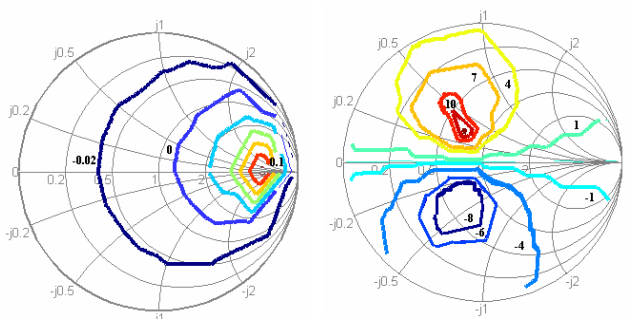


**Fig. 2:** $\Delta IM_3$ as a function of the base-band input (a) and output (b) terminations.

As a conclusion, output base-band termination, and in particular its imaginary part, acts as a multiplicative factor for $\Delta IM_3$ and its sign is the opposite of IMD asymmetry.

A further investigation is possible via the developed Volterra approach regarding the effect of the tones' spacing $\Delta\omega$ on $\Delta IM_3$, holding constant the *numerical values* of all harmonic impedances (base-band included). As a result, $\Delta IM_3$ is not (analytically) affected by $\Delta\omega$ value, even if a variation on $\Delta IM_3$ has been experimentally evidenced varying $\Delta\omega$ [1,4]. Nevertheless, it must be stressed that in real experiments a variation on $\Delta\omega$ usually implies a variation on base-band terminations too. Therefore, to account for such phenomena, and in particular for the variation of output base-band termination, $\Delta IM_3$ has been analysed assuming for the drain bias network a frequency behaviour similar to the ones reported in [4]. The resulting $\Delta IM_3$ values are depicted in Fig. 3, showing a similar behaviour with measurements [4] and demonstrating the validity of the approach.

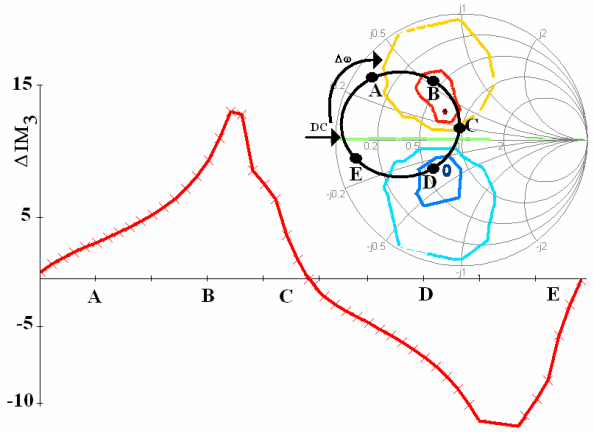


**Fig. 3:** $\Delta IM_3$ as a function of an output base-band termination as in the inset.

*B. Simplified Model*

The complete model can be simplified if a step-by-step investigation of IMD generation phenomena is carried out, replacing the respective nonlinear equivalent circuit element with its linear counterpart and observing the effect on third-order IMD and its asymmetry. In particular, contour plots of $\Delta IM_3$ in the same operating conditions adopted to generate Fig. 2b are reported in Fig. 4, neglecting non linearities related to gate and drain charge functions ( $Q_g$ and $Q_d$ respectively) and replacing

them with their linear capacitive counterparts. As it can be noted, "full non linear" and "simplified" models exhibit a similar qualitative behaviour.

As a consequence, for $\Delta IM_3$ evaluation purposes, a simplified non linear model with only non linear current source $I_{ds}$ can be adopted. The goal is to derive closed-form relationships to clarify the effects of base-band terminations on the IMD asymmetry.

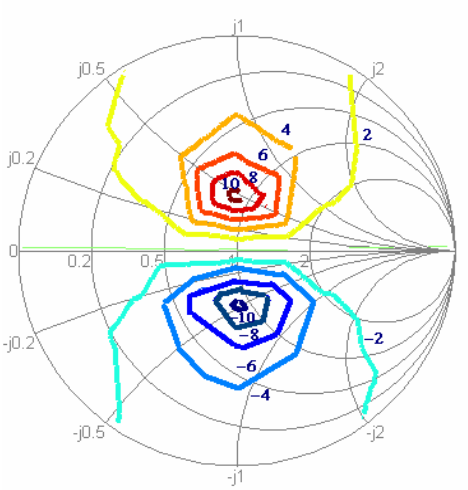


**Fig. 4:** $\Delta IM_3$ as a function of output base-band termination neglecting the nonlinearities associated to $Q_g$ and $Q_d$.

## III. Simplified Volterra Analysis

Assuming a two-tone input excitation, from Volterra analysis easily arises that upper and lower third-order IMD products are related to the kernels $H_3(\omega_2,\omega_2,-\omega_1)$ and $H_3(\omega_1,\omega_1,-\omega_2)$ respectively (as stated by (5)). These non linear functions $H_3$ differ for the presence of terms $H_2(\omega_2,-\omega_1)$ (in the $H_3$ upper) or $H_2(\omega_1,-\omega_2)$ (in the $H_3$ lower). The difference between such second-order kernels can be expressed as:

$$\Delta H_2 = H_2(\omega_2,\omega_2,-\omega_1) - H_2(\omega_1,\omega_1,-\omega_2) = \\ = j2B_{L,\Delta\omega}\cdot\frac{g_{m2}|Y_L|^2 + g_m\cdot(g_m g_{d2} - g_{md}G_L)}{|Y_L|^2\cdot|Y_{L,\Delta\omega}|^2} \qquad (6)$$

where $Y_{L,\Delta\omega} = G_{L,\Delta\omega} + jB_{L,\Delta\omega}$ is the base-band load admittance, and $Y_L = G_L + jB_L$ is the fundamental frequency load admittance. Symbolically, for $H_3$:

$$H_3(\omega_2,\omega_2,-\omega_1) = C(.) + N(\Delta\omega) \\ H_3(\omega_1,\omega_1,-\omega_2) = C(.) + N(-\Delta\omega) \qquad (7)$$

where

$$N(\Delta\omega) = \frac{-2y_{11}(\omega)}{3D(\omega)}\cdot\left\{\begin{matrix}2g_{d2}\cdot[H_2(\omega_2,-\omega_1)\cdot H_1(\omega_2)]+\\ +g_{md}\cdot[H_2(\omega_2,-\omega_1)]\end{matrix}\right\} = \\ = \frac{2\left\{\begin{matrix}(g_{md}Y_L - 2g_{d2}g_m)\cdot\\ \cdot\left[g_{m2}|Y_L|^2 + g_m\cdot(g_m g_{d2} - g_{md}G_L)\right]\end{matrix}\right\}}{3\cdot Y_{L,\Delta\omega}\cdot Y_L^2\cdot|Y_L|^2} \qquad (8)$$

thus obtaining, for $\Delta H_3$:

$$\Delta H_3 = N(\Delta\omega) - N(-\Delta\omega) = \qquad (9) \\ = \frac{-2y_{11}(\omega)\cdot\Delta H_2}{3\cdot D(\omega)}\cdot\left(g_{md} - 2g_{d2}\frac{g_m}{Y_L}\right) = \\ = \frac{-j4B_{L,\Delta\omega}\cdot\left\{\begin{matrix}(g_{md}Y_L - 2g_{d2}g_m)\cdot\\ \cdot\left[g_{m2}|Y_L|^2 + g_m\cdot(g_m g_{d2} - g_{md}G_L)\right]\end{matrix}\right\}}{3\cdot Y_L^2\cdot|Y_L|^2\cdot|Y_{L,\Delta\omega}|^2}$$

Expression (9) justifies, in a simplified way, several effects previously observed. For instance, it can be easily inferred that if output base-band termination is purely resistive (i.e. $B_{L,\Delta\omega}=0$), no IMD asymmetry arises, as in Fig. 2b. On the other hand, (9) relates the IMD asymmetry to the sign of $B_{L,\Delta\omega}$.

Utilising a vector representations of $H_3$ components [7], when $B_{L,\Delta\omega}$ is negative, then the resulting vectors $H_3(\omega_2,\omega_2,-\omega_1)$ and $H_3(\omega_1,\omega_1,-\omega_2)$ behave as the ones depicted in Fig. 5a, showing a positive $\Delta IM_3$ value. On the contrary, when $B_L$ is positive, the situation depicted in Fig. 5b arises, resulting in a negative $\Delta IM_3$.

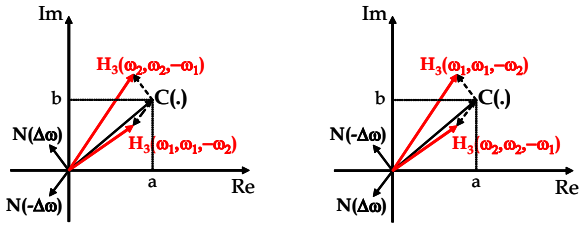


**Fig. 5:** Vector representation of upper and lower sideband $H_3$ kernels, for negative (a) and positive (b) equal $B_L$ values.

It is therefore possible to show analytically through expression (9), the IMD asymmetry generation and the key role of drain base-band termination.

To analyze however the role of the output fundamental and second harmonic terminations, it is necessary to directly analyse $\Delta IM_3$ , as defined in (4).

Under the hypothesis of a unilateral nonlinear device circuit model, characterized by the nonlinear controlled current source $I_{ds}$ only, the complete expression for $\Delta$ is derived. Such expression involves all nonlinear $I_{ds}$ expansion parameters :

$$\Delta = \frac{-8B_{L,\Delta\omega}\cdot(F_1+F_2)\cdot\left[\begin{matrix}g_{m2}|Y_L|^2 +\\ +g_m\cdot(g_m g_{d2} - g_{md}G_L)\end{matrix}\right]}{9\cdot|Y_{L,\Delta\omega}|^2\cdot|Y_{L,2}|^2\cdot|Y_L|^8} = \qquad (10) \\ = \frac{-4\cdot(F_1+F_2)\cdot Im\{\Delta H_2\}}{9\cdot|Y_{L,2}|^2\cdot|Y_L|^6}$$

where $Y_{L,2} = G_{L,2} + jB_{L,2}$ is the load admittance at second harmonic frequency and $F_1$ and $F_2$ are respectively given by:

$$F_1 = \begin{bmatrix} g_m B_L^3 \cdot \begin{pmatrix} \left|Y_{L,2}\right|^2 \cdot \left(6 g_{d2} g_{m3} - g_{m2d} g_{md}\right) + \\ -G_{L,2} g_{md} \cdot \left(4 g_{d2} g_{m2} - g_{md}^2\right) \end{pmatrix} + \\ -B_{L,2} B_L^4 g_{md}^2 g_{m2} + \\ +B_{L,2} B_L^2 \cdot \begin{pmatrix} g_{m2} g_{md} G_L \cdot \left(4 g_{d2} g_m - 2 G_L g_{md}\right) + \\ +g_{d2} g_m^2 \cdot \left(4 g_{d2} g_{m2} - 3 g_{md}^2\right) + \\ +G_L g_m g_{md}^3 \end{pmatrix} \end{bmatrix} \quad (11)$$

$$F_2 = \begin{bmatrix} B_L \cdot \begin{pmatrix} \left|Y_{L,2}\right|^2 \cdot \begin{pmatrix} 2 g_m^2 g_{md2} \cdot \begin{pmatrix} g_m g_{d2} + \\ +G_L g_{md} \end{pmatrix} + \\ +G_L^2 g_m \cdot \begin{pmatrix} 6 g_{d2} g_{m3} + \\ -g_{md} g_{m2d} \end{pmatrix} + \\ -g_m^2 \cdot \begin{pmatrix} 3 g_m g_{md} g_{d3} + \\ +4 G_L g_{d2} g_{m2d} \end{pmatrix} \end{pmatrix} + \\ +G_{L,2} g_m G_L \cdot \begin{pmatrix} \left(g_{md}^2 - 4 g_{m2} g_{d2}\right) \cdot \\ \cdot \left(G_L g_{md} - 2 g_m g_{d2}\right) \end{pmatrix} \end{pmatrix} + \\ -B_{L,2} \cdot \begin{pmatrix} G_L^4 g_{m2} g_{md}^2 - G_L^3 g_m g_{md} \cdot \left(g_{md}^2 + 4 g_{m2} g_{d2}\right) + \\ +G_L^2 g_m^2 g_{d2} \cdot \left(5 g_{md}^2 + 4 g_{m2} g_{d2}\right) + \\ +4 g_m^3 g_{d2}^2 \cdot \left(g_m g_{d2} - 2 G_L g_{md}\right) \end{pmatrix} \end{bmatrix} \quad (12)$$

Expression (10) can be further simplified, resulting in (13), if the higher order terms for $g_d$ (namely $g_{d2}$ and $g_{d3}$) are neglected together with third-order cross terms (namely $g_{md2}$ and $g_{m2d}$). From the latter expression a few further remarks can be carried out: power IMD asymmetry arises if the base-band output admittance exhibits an imaginary part (as already recognised from [7]); however, it is also necessary that the output terminations exhibit an imaginary part at fundamental and/or second harmonic frequencies. In fact, it can be noted that $\Delta IM_3=0$ if $B_L= B_{L,2}=0$ even if $B_{L,\Delta\omega}$ is not nulled. The major role in IMD asymmetry is clearly played by $g_{md}$ whose value is directly related to the asymmetry magnitude.

$$\Delta IM_3 = \frac{\left(\frac{3}{4}A^3\right)^2 Re\{Y_L\}}{2} \cdot \\ -\frac{8}{9} B_{L,\Delta\omega} g_{md}^2 \begin{bmatrix} \left(g_{m2}\left|Y_L\right|^2 - g_{md} g_m G_L\right) \cdot \\ \cdot \begin{pmatrix} g_{md} g_m \cdot \left(G_{L,2} B_L + G_L B_{L,2}\right) \\ -B_{L,2} g_{m2} \left|Y_L\right|^2 \end{pmatrix} \end{bmatrix} \cdot \\ \cdot \frac{}{\left|Y_L\right|^6 \cdot \left|Y_{L,2}\right|^2 \cdot \left|Y_{L,\Delta\omega}\right|^2} = \\ = \frac{\left(\frac{3}{4}A^3\right)^2 Re\{Y_L\}}{2} \cdot \\ -\frac{4}{9} g_{md}^2 \cdot \begin{bmatrix} Im\{\Delta H_2\} \cdot \\ \cdot \begin{pmatrix} g_{md} g_m \cdot \left(G_{L,2} B_L + G_L B_{L,2}\right) + \\ -B_{L,2} g_{m2} \left|Y_L\right|^2 \end{pmatrix} \end{bmatrix} \\ \cdot \frac{}{\left|Y_L\right|^4 \cdot \left|Y_{L,2}\right|^2} \quad (13)$$

Finally, from expression (13), a potential null for IMD asymmetry is possible, if proper second-harmonic load is selected. In fact, with a given fundamental-frequency load, IMD asymmetry cancellation results if the following condition holds:

$$B_{L,2} = \frac{g_m G_{L,2} g_{md} B_L}{g_{m2}\left|Y_L\right|^2 - g_{md} g_m G_L} \quad (14)$$

## IV. Conclusions

In this contribution, a study on IMD asymmetry has been carried out, trying to clarify the effects of active device terminations on IMD asymmetry generation. Through a full nonlinear device model, the effects of output base-band termination have been analysed. These simulations underline the basic role in IMD asymmetry generation played by the reactive behaviour of output base-band load through the nonlinearities associated to the current source. Finally, through a Volterra series and a simplified model, a symbolic expression for IMD asymmetry has been derived, evidencing the effects of fundamental and second harmonic terminations.


## Acknowledgement

Research reported here was performed in the context of the network TARGET– "Top Amplifier Research Groups in a European Team" and supported by the Information Society Technologies Programme of the EU under contract IST-1-507893-NOE, www.target-net.org


## References


[1] Y.Wang, S.V.Cherepko and J.C.M.Hwang, "Asymmetry in intermodulation distortion of HBT Power Amplifiers", IEEE GaAs Digest, pp 201-204, 2001.

[2] J.F.Sevic, K.L.Burguer and M.B.Steer, "A novel envelope-termination load-pull methods for ACPR optimization of RF/microwave power amplifiers", in IEEE MTT-S Int. Microwave Symp. Dig., Baltimore, MD, 1998, pp 601-605.

[3] B.De Carvalho, J.C.Pedro, "Two-Tone IMD Asymmetry in Microwave Power Amplifier," IEEE MTT-S Symposium Digest, 2000.

[4] B.De Carvalho, J.C.Pedro, "Comprehensive explanation of distortion sideband asymmetries", IEEE Trans. Microwave Theory Tech., vol. 50, no 9, Sept. 2002.

[5] P.Colantonio, F.Giannini, E.Limiti, A.Nanni, "Distortion Sideband Asymmetries in Power Amplifier through Volterra series", INMMIC Workshop, Rome, Nov. 2004, pp 601-605.

[6] F.Giannini, G.Leuzzi, G.Orengo, P.Colantonio, "Modeling Power and Intermodulation Behavior of Microwave Transistors with Unified Small-Signal/Large-Signal Neural Network Models," International Journal of RF and Microwave Computer-Aided Engineering, Vol.13, N°4, July 2003, pp. 276-284.

[7] J.Brinkhoff, and A.E.Parker, "Effect of Baseband Impedence on FET Intermodulation", IEEE Trans. Microwave Theory and Tech., vol. 51, NO. 3, pp 1045-1051, March 2003.